# Determination of the Structure and Chiroptical Properties of the Parent Nerve Gas *O*-Methyl Methylphosphonofluoridate by ab Initio Calculations, Electron Diffraction Analysis, and NMR Spectroscopy

**A. Rauk,*,† I. F. Shishkov,‡ L. V. Vilkov,‡ K. F. Koehler,§ and R. G. Kostyanovsky⊥**

*Contribution from the Department of Chemistry, The University of Calgary, Calgary, Alberta, Canada T2N 1N4, Department of Chemistry, Moscow State University, 119899 Moscow GSP-3, B-234, Russia, Gesellschaft fur Beseitigung von Kampfmitteln, Kampfstoffen, Kampstoffmunition, Dr. Koehler GmbH, Barbarahof, Kreutsen, D-3042 Munster, Germany, and N. N. Semenov Institute of Chemical Physics, Russian Academy of Sciences, 4 ul. Kosygina, 117977 Moscow, Russia*

*Received January 26, 1995*[⊗]

**Abstract:** The geometry and electronic structure of *O*-methyl methylphosphonofluoridate (**1**) (MeOPOFMe) have been determined at the MP2/6-31G(D) and Becke3LYP/6-31G(D) levels. The calculations confirm the prior results of lower-level ab initio calculations which indicated that the experimental gas phase electron diffraction structure of **1** is substantially in error. The compound exists in a single conformation determined by the operation of an anomeric effect between the methoxy oxygen atom and the P−F bond as is evident from the nearly perpendicular orientation of the O−C and P−F bonds. A reanalysis of the published gas electron diffraction (GED) data yielded inconclusive results but underscored the inability of GED to distinguish between the conformations of **1**. $^{1}H$ and $^{13}C$ NMR spectra are reported and are consistent with the existence of a single conformer. The lower excited singlet states of **1** are calculated to be Rydberg states originating from excitations from the *p*-type nonbonding orbitals of the monocoordinated oxygen atom into diffuse 3s- and 3p-type orbitals. The transitions are predicted to occur in the vacuum UV and have low oscillator strength. The first two transitions have moderate positive rotatory strength for the (*R*) enantiomer, leading to the prediction of absolute configuration, (+)-(*R*)-**1**.

## Introduction

Compounds of the general structure

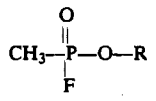

**1** R = $CH_3$
**2** R = $CH(CH_3)_2$ sarin (GB)
**3** R = $CH(CH_3)C(CH_3)_3$ soman (GD)

are potent anticholinesterases and have been produced as chemical warfare nerve gas agents. Sarin (**2**) has been found to have high mutagenic activity.[1] The compounds interest us since they provide the opportunity to make correlations between biological activity and absolute and relative chirality. The stereoisomeric forms are readily distinguished in NMR spectroscopy by the use of chiral shift reagents.[2] The four stereoisomers of soman (**3**) have been separated and found to differ in anticholinesterase activity by up to 105-fold, and in acute toxicity by up to 100-fold from the least toxic to the most.[3] The absolute configuration (*S*)-(−) at the chiral phosphorus center for the most active forms has been determined from analysis of NMR coupling constants of the two diastereomeric forms of soman (**3**).[4] The same absolute (*S*)-(−) configuration for the more toxic enantiomer of sarin (**2**) was suggested on the basis of chemical correlation.[3] The absolute configuration of the parent **1** is not known. Indeed, no spectroscopic chiroptical properties have been published for **1** or any other of this class of anticholinesterases.

Several experimental[5] and theoretical investigations[6−9] of the structure and electrostatic properties of chemical nerve agents, including the parent compound *O*-methyl methylphosphonofluoridate (**1**), have been reported. The experimental structure of **1** has been determined by Zeil and co-workers from gas phase electron diffraction analysis (GED),[5] but has been questioned on the basis of ab initio RHF/STO-3G* and RHF/3-21G* computations.[7] Significant differences were found between experimental and calculated values for all parameters. In particular, a significant difference was noted for the predicted conformation. According to the GED study, the major conformer has the methoxy group approximately anticoplanar to the P=O bond and *gauche* to the methyl and fluorine atoms (Chart 1, conformer **b**) while the single stable conformer predicted by the RHF/3-21G* calculations is a structure with

† The University of Calgary.
‡ Moscow State University.
§ Gesellschaft fur Beseitigung von Kampfmitteln.
⊥ Russian Academy of Sciences.
⊗ Abstract published in *Advance ACS Abstracts*, June 15, 1995.

(1) Rapoport, I. A.; Kostyanovsky, R. G. *Dokl. Akad. Nauk SSSR* **1960**, *131*, 191−194; *Dokl. Chem. (Trans. of Dokl. Akad. Nauk)* **1960**, *131*.
(2) (a) Van den Berg, G. R.; Beck, H. C.; Benschop, H. P. *Bull. Environ. Contam. Toxicol.* **1984**, *33*, 505; *Chem. Abstr.* **1985**, *102*, 18994m. (b) Miao, Z.; Du, Z. *Bopuxue Zazhi* **1989**, *6*, 469; *Chem. Abstr.* **1990**, *112*, 133925h.
(3) Benshop, N. P.; De Jong, L. P. A. *Acc. Chem. Res.* **1988**, *21*, 368.
(4) Koehler, K. F.; Zaddach, H.; Kuntsevich, A. D.; Chervin, I. I.; Kostyanovsky, R. G. *Russ. Chem. Bull.* **1993**, *42*, 1611−1612.
(5) Zeil, W.; Krutz, H.; Haase, J.; Oberhammer, H. *Z. Naturforsch.* **1973**, *28a*, 1717.
(6) Politzer, P.; Jayasuriya, K. *J. Mol. Struct.: THEOCHEM* **1986**, *134*, 381.
(7) Ewig, C. S.; Van Wazer, J. R. *J. Mol. Struct.: THEOCHEM* **1985**, *122*, 179−187.
(8) Politzer, P.; Jayasuriya, K.; Lane, P. *J. Mol. Struct.: THEOCHEM* **1987**, *34*, 259.
(9) Hariharan, P. C.; Lewchenko, V.; Koski, W. S.; Kaufman, J. J. *Int. J. Quantum Chem., Quantum Biol. Symp.* **1982**, *9*, 259.

0002-7863/95/1517-7180$09.00/0 

**Chart 1**

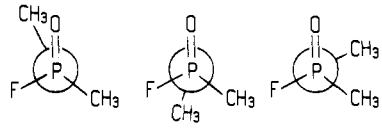

**a** **b** **c**

RHF/3-21G*(ref 7) GED (ref 5) NMR of 3 (ref 4)

the two methyl groups approximately *anti* to each other making a dihedral angle between the P=O and O—Me bonds of only 16.5° (Chart 1, conformer **a**). The matter is further complicated by the recent analysis of the NMR spin—spin coupling constants of soman (**3**). A large $^4J_{CF}$ coupling constant, 1.5 Hz, between the quarternary C atom of the *tert*-butyl group and the fluorine atom is observed only in the most stable diastereomer. This strongly implies a W conformation of the four bonds, and in particular suggests that the alkyl group of the alkoxy moiety adopts a position anticoplanar to the fluorine atom. Notwithstanding that soman is a more complex system, in the context of **1**, the NMR study implies that a conformation with the methyl of the methoxy group anticoplanar to fluorine (Chart 1, conformer **c**) must be considered.

Here we report the results of high-level ab initio computations aimed at determining the stable conformation(s) of **1**, together with a detailed analysis of the NMR spectrum. In addition, a reanalysis of the GED data of Zeil et al.[5] is attempted. Finally, the chiroptical properties of the lower electronic states are predicted on the basis of perturbative CI calculations.

## Computational Methods

The structures of methylphosphonofluoridate **1** were fully optimized at the Hartree—Fock (RHF), second-order Moller—Plesset (MP2), and density functional theoretical levels using procedures implemented in the Gaussian 92/DFT system of programs,[10] and the internal 6-31G-(D) basis set. In the case of the MP2 calculations, the frozen core approximation was used.

For the DFT calculations, a hybrid approach based on Becke's three-parameter functional[11] was employed (Becke3LYP). The functional form is

$$(1 - a_0)E_X^{LSDA} + a_0E_X^{HF} + a_X\Delta E_X^{B88} + a_CE_C^{LYP} + (1 - a_C)E_C^{VWN}$$

where the energy terms are the Slater exchange, the Hartree—Fock exchange, Becke's 1988 exchange functional correction,[12] the gradient-corrected correlation functional of Lee, Yang, and Parr,[13] and the local correlation functional of Vosko, Wilk, and Nusair,[14] respectively. The values of the coefficients determined by Becke are

$$a_0 = 0.20, \quad a_X = 0.72, \quad a_C = 0.81$$

The complete potential curve for rotation about the P—O bond was characterized at the Becke3LYP/6-31G(D) level by geometry optimization with the C—P—O—C dihedral angle fixed at 15° intervals.

Chiroptical properties were calculated using the 6-31+G(D) basis set at the MP2/6-31G(D) geometries. The use of the diffuse s and p functions designated by the "+" is desirable for a more accurate description of the excited singlet states which tend to be more diffuse than the ground state. For chiroptical properties, the PCI program was used. The PCI program determines optical rotatory strengths and dipole oscillator strengths from electric and magnetic dipole transition moments which are correct to first order in Rayleigh—Schrödinger perturbation theory. Both the ground state and excited states are partitioned into zero-order (strongly interacting) and first-order (weakly interacting) contributions. Only single excitation CI is carried out for the excited states selected from a window of 15 occupied and 50 unoccupied MOs. Electron correlation of the ground state wave function is taken into account in the form of doubly excited configurations (generated within the same window) as first-order corrections to the zero-order Hartree—Fock single determinantal wave function. PCI has been extensively used,[15] and the theory is described in detail elsewhere.[16]

## Experimental Section

The NMR spectra were measured on a Bruker WM-400 spectrometer ($^1$H, 400.1 MHz; $^{13}$C, 100.6 MHz; $^{19}$F, 376.5 MHz; $^{31}$P, 162.0 MHz), the UV spectrum was measured on a Specord UV—vis spectrophotometer, the CD spectrum was recorded on a JASCO J-500A spectropolarimeter, and optical rotation was recorded on a Polamat A polarimeter.

*O*-Methyl methylphosphonofluoridate (**1**) was prepared by using the established method for other *O*-alkyl methylphosphonofluoridates.[17] A solution of MeOH (0.65 g, 20 mmol) in 10 mL of $CH_2Cl_2$ was added to a mixture of $MeP(O)F_2$ (1 g, 10 mmol) and $MeP(O)Cl_2$ (1.3 g, 10 mmol) in 50 mL of $CH_2Cl_2$ at 0 °C. After the solution stood at room temperature for 24 h the solvent was evaporated in vacuo (100 Torr), and the product was distilled. Yield of **1**: 1.1 g (98%). Bp: 80—82 °C, 100 Torr. $^1$H NMR spectrum ($C_6D_6$, from TMS) ($\delta$, ppm) ($J$, Hz): 1.14 (dd, 3H, MeP, $^2J_{HP} = 18.6$, $^3J_{HF} = 5.8$); 3.47 (dd, 3 H, MeO, $^3J_{HP} = 11.4$, $^4J_{HF} = 0.8$). $^{13}$C NMR spectrum ($C_6D_6$, from TMS) ($\delta$, ppm) ($J$, Hz): 9.28 (ddq, MeP, $^1J_{CH} = 129.6$, $^1J_{CP} = 147.8$, $^2J_{CF} = 27.4$); 52.86 (dq, MeO, $^1J_{CH} = 148.9$, $^2J_{CP} = 6.8$). $^{19}$F NMR spectrum ($C_6D_6$, from $CF_3COOH$ external) ($\delta$, ppm) ($J$, Hz): 16.4 (dqq, $^1J_{FP} = 1045.0$). $^{31}$P NMR spectrum ($C_6D_6$, from $H_3PO_4$ external) ($\delta$, ppm) ($J$, Hz): 32.4 (dqq, $^1J_{PF} = 1045.0$, $^2J_{PH} = 18.6$, $^3J_{PH} = 11.4$). In the UV spectrum of **1** in *n*-hexane there is no maximum in the absorption curve up to 190 nm, in agreement with the data for **2** and **3**.[18]

(−)-*O*-Bornylmethylphosphonofluoridate was obtained by using the same method from (−)-borneol. Yield: 70%. $[\alpha]^{20}_D$: −8.3° (*c* 3.2, *n*-hexane). The ratio of diasteromers was determined from the relative intensities of the signals in the $^{13}$C NMR spectrum ($CDCl_3$, from TMS) ($\delta$, ppm) ($J$, Hz): (for the major diasteromer) 9.6 (ddq, MeP, $^1J_{CH} = 126.4$, $^1J_{CP} = 149.7$, $^2J_{CF} = 27.6$), 84.14 (ddd, CHO $^1J_{CH} = 152.6$, $^2J_{CP} = 7,7$, $^3J_{CF} = 1.8$); (for the minor diastereomer) 9.48 (ddq, MeP, $^1J_{CH} = 126.4$, $^1J_{CP} = 150.0$, $^2J_{CF} = 27.7$), 83.70 (ddd, CHO $^1J_{CH} = 152.6$, $^2J_{CP} = 7.6$, $^3J_{CF} = 1.5$). In the CD spectrum of this compound, no Cotton effect is observed up to 190 nm.

## Results and Discussion

**Ab Initio Calculations.** At each of the three levels of theory, two conformations, **1a** and **1b** (Figure 1; see also Chart 1), were found, separated by approximately 3 kcal mol$^{-1}$, with **1a** lower in energy. The total energies are listed in Table 1. Structure **1a** is essentially the same as that found in the earlier ab initio study at the RHF/3-21G* level.[7] The second structure, **1b**,

(10) Frisch, M. J.; Trucks, G. W.; Head-Gordon, M.; Gill, P. M. W.; Wong, M. W.; Foresman, J. B.; Johnson, B. G.; Schlegel, H. B.; Robb, M. A.; Replogle, E. S.; Gomperts, R.; Andres, J. L.; Raghavachari, K.; Binkley, J. S.; Gonzalez, C.; Martin, R. L.; Fox, D. J.; Defrees, D. J.; Baker, J.; Stewart, J. J. P.; Pople, J. A. *Gaussian 92*, Revision B; Gaussian, Inc.: Pittsburgh, PA, 1992.

(11) Becke, A. D. *J. Chem. Phys.* **1993**, *98*, 5648.

(12) Becke, A. D. *Phys. Rev. A* **1988**, *38*, 3098.

(13) Lee, C.; Yang, W.; Parr, R. G. *Phys. Rev. B* **1988**, *37*, 785.

(14) Vosko, S. H.; Wilk, L. Nusair, M. *Can. J. Phys.* **1980**, *58*, 1200.

(15) (a) Shustov, G. V.; Varlamov, S. V.; Rauk, A.; Kostyanovsky, R. G. *J. Am. Chem. Soc.* **1990**, *112*, 3403—3408. (b) Shustov, G. V.; Kadorkina, G. K.; Varlamov, S. V.; Kachanov, A. V.; Kostyanovsky, R. G.; Rauk, A. *J. Am. Chem. Soc.* **1992**, *114*, 1616—1623. (c) Shustov, G. V.; Kadorkina, G. K.; Kostyanovsky, R. G.; Rauk, A. *J. Am. Chem. Soc.* **1988**, *110*, 1719—1726. (d) Shustov, G. V.; Kachanov, A. V.; Kadorkina, G. K.; Kostyanovsky, R. G.; Rauk, A. *J. Chem. Soc., Chem. Commun.* **1992**, 705—706. (e) Shustov, G. V.; Kachanov, A. V.; Kadorkina, G. K.; Kostyanovsky, R. G.; Rauk, A. *J. Am. Chem. Soc.* **1992**, *114*, 8257—8262. (f) Shustov, G. V.; Varlamov, S. V.; Rauk, A.; Kostyanovsky, R. G. *J. Am. Chem. Soc.* **1990**, *112*, 3403. (g) Rauk, A. *J. Am. Chem. Soc.* **1984**, *106*, 6517—6524.

(16) Rauk, A.; Barriel, J. M. *Chem. Phys.* **1977**, *25*, 409—424.

(17) Schmutzler, R. In *Advances in Fluorine Chemistry*; Stacey, M. Tatlow, J. C., Sharple, A. G., Eds.; Butterworth: London, 1965; Vol. 5, p 31.

(18) Rewick, R. T.; Schumacher, M. L.; Haynes, D. L. *Appl. Spectrosc.* **1986**, *40*, 152—156.

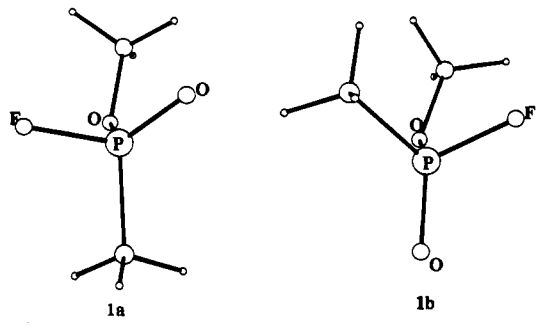


1a 1b

**Figure 1.** Ab initio structures of the two comformers of *O*-methyl (*R*)-methylphosphonofluoridate (**1**). See Table 2 for values of the geometric parameters.

**Table 1.** Absolute and Relative Energies of Structures **1a** and **1b**

| method | $E$(**1a**)[a] | $E$(**1b**)[a] | $\Delta E$[b] |
|---|---|---|---|
| RHF/6-31G(D) | −669.205 71 | −669.199 53 | 3.9 |
| MP2(FC)/6-31G(D) | −670.105 21 | −670.099 28 | 3.7 |
| Becke3LYP/6-31G(D) | −671.546 78 | −671.541 29 | 3.4 |
| Becke3LYP/6-311G(2DF,P)[c] | −671.718 61 | −671.714 53 | 2.6 |

[a] In hartrees. [b] Energy of **1b** relative to **1a**, in kilocalories per mole. [c] Becke3LYP/6-31G(D) geometry.

superficially resembles the experimental structure of Zeil et al.[5] but differs substantially in detail. The DFT energy was reevaluated using the 6-311G(2DF,P) basis set by single-point calculations of the 6-31G(D) geometries. At this highest level, structure **1a** is predicted to be more stable than **1b** by 2.6 kcal mol$^{-1}$. All levels were employed in the search for a third staggered conformation, **1c**, but in each case, optimization from a reasonable representation of **1c** yielded, without activation, the minimum energy structure **1a**.

The potential curve for rotation about the P−O bond as a function of the C−P−O−C dihedral angle is shown in Figure 2. Structure **1c** (Chart 1), which corresponds to a point at which the C−P−O−C torsion angle is 300°, is seen not to be a local minimum.

Selected geometric details are listed in Table 2. Listed for comparison are the data of Zeil and co-workers.[5] As can be seen from the data (Tables 1 and 2), the Becke3LYP procedure produces geometries and relative energies that are very similar to those from the MP2 method, but with substantially less computational effort. The largest difference in bond length occurs for the P−C bond and is only 0.013 Å. The largest deviation in bond angles and dihedral angles is 2°.

The lower energy conformation has a nearly perpendicular orientation of the P−F bond with the C−O−P plane (dihedral angle FPOC, Figure 1, Table 2). The presence of the perpendicular orientation is suggestive of, and attributable to, the operation of an anomeric interaction. The energetically favorable anomeric interaction[19] is the interaction between the higher nonbonded electron pair of the dicoordinated oxygen ($n_O$) and the low-lying antibonding orbital of the P−F bond ($\sigma_{PF}$*). The interaction is strongest when the $n_O$ (a p orbital perpendicular to the plane of the bonds to the dicoordinated oxygen atom) and $\sigma_{PF}$* orbitals are oriented in the same plane, i.e., when the O−C and P−F bonds have a nearly perpendicular arrangement.[20]

(19) (a) Radom, L.; Hehre, W. J.; Pople, J. A. *J. Am. Chem. Soc.* **1972**, *94*, 2371. (b) Rauk, A. *Orbital Interaction Theory of Organic Chemistry*; Wiley-Interscience: New York, 1994.

(20) The anomeric interactions (also called negative hyperconjugation) between the nonbonded electron pairs of the monocoordinated oxygen atom and the antibonding orbitals, $\sigma_{PF}$* and $\sigma_{PO}$*, may be even stronger but are not expected to influence the angle of rotation about the P−O bond.

In the second conformation, which is about 3 kcal mol$^{-1}$ less stable, the FPOC dihedral angle is approximately 35°, evidently due to a severe steric interaction of the two methyl groups, and the anomeric effct is strongly attenuated. A third staggered structure, **1c**, in which the P−F and O−C bonds are anticoplanar is not a stationary point and is also predicted to be 3 kcal mol$^{-1}$ higher in energy (Figure 2). The energy difference may be taken as a measure of the energetic advantage of the anomeric effect. This question was explored further by optimization of two structures with the F atom constrained to lie in the C−O−P plane, namely, with ∠FPOC = 0° and 180°. In neither of these structures is negative hyperconjugation of the ether oxygen with the P−F bond (i.e., the anomeric effect) possible. The energies relative to **1a** are 3.7 and 2.8 kcal mol$^{-1}$, respectively.

**NMR Coupling Constant Analysis.** The $^{13}$C and $^{19}$F NMR spectra of **1** are shown in Figure 3. The predicted gas phase structure **1a** is expected to be the same as the structure in $C_6D_6$ solution in view of the nonpolar nature of $C_6D_6$ and the shape of the rotational curve (Figure 2). Two experimental observations bear directly on the solution conformation of **1**, namely, the observation of four-bond spin−spin coupling between the MeO hydrogen atoms and the fluorine atom in the $^1$H and $^{19}$F spectra ($^4J_{HF}$ = 0.8 Hz, Figure 3b), and the *lack* of an observable three-bond spin−spin coupling between the MeO carbon atom and fluorine in the $^{13}$C spectrum ($^3J_{CF}$ not observed, Figure 3a). If, as is generally supposed on the basis of HH coupling, a planar configuration of bonds is required for long-range coupling, then the lack of observable MeO carbon to fluorine coupling is consistent with the predicted structure, **1a**, since the torsion angle of the relevant bonds (angle FPOC, Figure 1) is close to 90°. Two possible interpretations remain for the observation of long-range coupling between the MeO hydrogen atoms and the fluorine atom: (a) the mechanism of coupling is not through bonds but rather through space, or (b) the mechanism is through bonds, the transmission of coupling information being facilitated by the $n_O$−$\sigma_{PF}$* interaction associated with the anomeric effect; i.e., a coplanar geometry is not required.

**Reanalysis of the GED Data of Zeil et al.[5]** The analysis of the results of the electron diffraction study of **1** showed that the contribution of the interatomic distances as a function of the internal rotation about the P−O bond is very small. The similar values of the P=O, P−F, P−O, and C−O bonds led Zeil and co-workers to conclude that the reliability of the parameters determined is not very high because of the very strong correlation.[5] The main conclusion, namely, that the predominant conformer is **b** (Chart 1), is not supported by subsequent work. Some parameters were unreasonable, and an *R*-factor for internal consistency of the refinement was not provided. Therefore, we decided to repeat a refinement of the structure.

As the original data associated with the GED experiments are no longer available,[21] we digitized the published scattering pattern, $sM_{(s)}$, which spanned the range $S_{min}$ = 1 Å$^{-1}$ to $S_{max}$ = 27 Å$^{-1}$, and attempted the least squares refinement according to standard procedures.[22] The "experimental" radial distribution curve (E) derived from the digitized scattering pattern is shown in Figure 4a. The following bond lengths and bond angles were used for the description of the molecular geometry: $r$(P=O), $r$(P−O), $r$(P−F), $r$(C−O), $r$(P−C), $r$(C−H), ∠POC, ∠OPO, ∠CPO, ∠O=PF, ∠CPF. However, the *difference* between $r$(P−O) and each of $r$(P−O), $r$(P−F), and $r$(C−O) was assumed from the ab initio calculation (Table 2, **1a**, DFT). In addition,

(21) Oberhammer, H. Private communication, 1994.

(22) Andersen, B.; Seip, H. M.; Strand, T. G.; Stolevik, R. *Acta Chem. Scand.* **1969**, *23*, 3224.

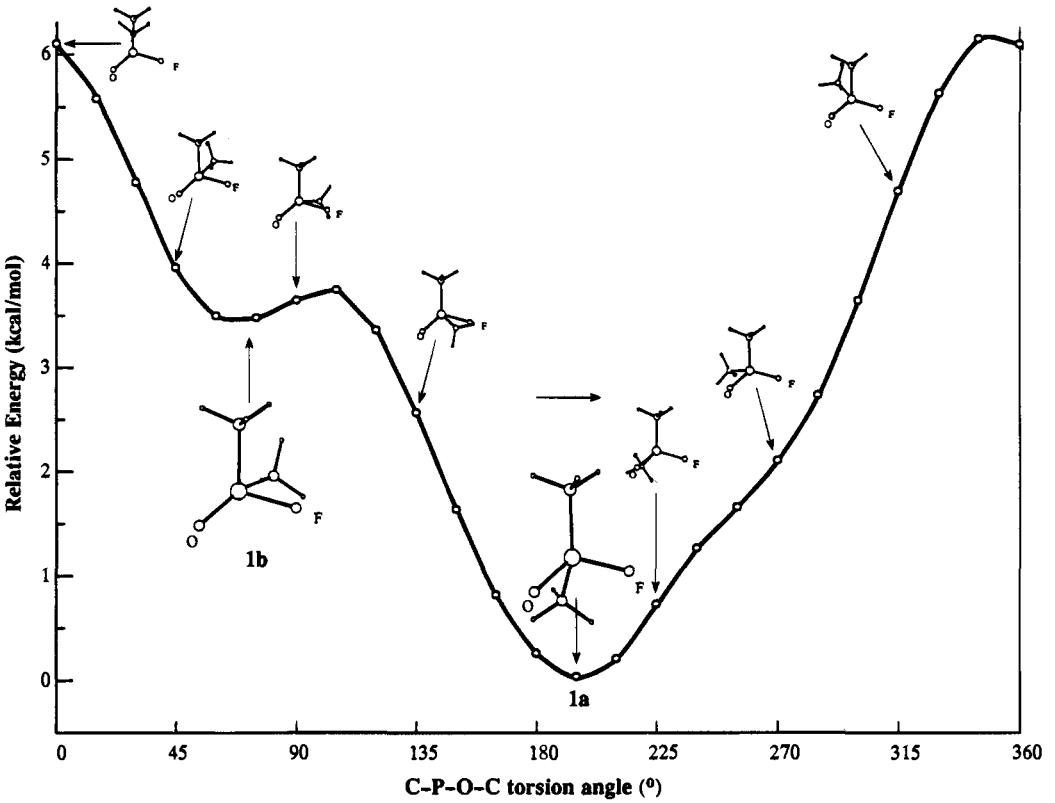


**Figure 2.** Potential curve for rotation about the P—O bond. The geometries were fully optimized at the Becke3LYP/6-31G* level except for the constraint of fixing the C—P—O—C torsion angle (Figure 1).

**Table 2.** Geometries of **1a** and **1b** with the 6-31G(D) Basis Set[a]

| | Ab initio | | | | ED | | | |
|---|---|---|---|---|---|---|---|---|
| | **1a** | | **1b** | | | present reanalysis (Chart 1)[c] | | |
| parameter | MP2 | DFT | MP2 | DFT | Zeil et al.[b] | **1a** | **1b** | **1c** |
| *r*(P—F) | 1.600 | 1.598 | 1.602 | 1.599 | 1.539(6) | 1.522(7) | 1.510(4) | 1.503(8) |
| *r*(P=O) | 1.481 | 1.477 | 1.475 | 1.471 | 1.489(6) | 1.486(4) | 1.492(7) | 1.496(9) |
| *r*(P—C) | 1.790 | 1.803 | 1.798 | 1.810 | 1.785(7) | 1.788(4) | 1.794(4) | 1.800(3) |
| *r*(P—O) | 1.610 | 1.609 | 1.610 | 1.609 | 1.552(6) | 1.594(5) | 1.597(4) | 1.610(3) |
| *r*(C—O) | 1.450 | 1.440 | 1.442 | 1.436 | 1.473(9) | 1.452[d] | 1.458[d] | 1.462[d] |
| ∠O=PF | 112.7 | 112.6 | 114.9 | 114.7 | 114.2 | 112.4(2.3) | 111.6(2.6) | 114.4(2.6) |
| ∠FPC | 102.0 | 102.0 | 101.2 | 101.4 | 100.5 | 98.3(7) | 99.6(1.4) | 100.0(1.7) |
| ∠FPO | 102.4 | 102.6 | 101.4 | 101.4 | 105.6(0.8) | 103.2(1.6) | 103.9(1.4) | 102.1(1.4) |
| ∠O=PC | 118.8 | 118.7 | 116.4 | 116.5 | 89.5 | | | |
| ∠OPO | 116.7 | 116.7 | 114.1 | 113.6 | 122.5(2.5) | 114.2(1.9) | 111.5(2.4) | 109.5(2.4) |
| ∠CPO | 101.9 | 102.1 | 107.0 | 107.3 | 123.5(1.8) | 108.7(1.0) | 109.3(7) | 109.0(1.2) |
| ∠POC | 117.6 | 119.6 | 121.4 | 123.0 | 116.3(0.9) | 119.6[e] | 119.6[e] | 119.6[e] |
| ∠FPOC | 88.2 | 90.2 | −34.4 | −36.7 | −3.2 | | | |
| ∠OPOC | −35.4 | −33.3 | −158.5 | −160.6 | −163.7 | | | |
| ∠CPOC[f] | 193.5 | 195.6 | 71.2 | 69.3 | 82.2 | 159.2(2.9) | 47.8(3.2) | 306.6(4.4) |
| *R*, % | | | | | | 12.2 | 12.5 | 11.9 |

[a] See Figure 1, bond lengths in angstroms, angles in degrees. [b] Reference 5. [c] See text. [d] Average difference between the bond lengths P=O and C—O was fixed at 0.034 Å from the ab initio DFT results. [e] Assumed. [f] ∠CPOC = 0 for the *syn* conformer (Figure 2).

some groups of amplitudes of the corresponding distances were varied. We tested three staggered conformers differing by the CPOC dihedral angle according to Chart 1. The E − T (experimental − theoretical) curves are shown in Figure 4a. The *R*-factor for structure **a** (Chart 1) was found to be 19.0%, **b** (Chart 1) gave 16.6%, and structure **c** (Chart 1) yielded 17.0%. However, no statistical significance could be attached to differences between these numbers on the basis of the available graphical data. Values of ∠CPOC for the three models (1) were (**a**) 173.4°, (**b**) 48.0°, and (**c**) 300°.

It is apparent from observation of the difference curves, E − T (Figure 4a) that we have three different intervals. In the first, less than 1.2 Å, a large disagreement with the experimental curve is found. For the C—H peak we fixed the amplitude at the reasonable value 0.075 Å rather than the value 0.019 Å of Zeil and co-workers, which was obtained by refinement. We considered the value 0.019 to be too small in comparison to C—H amplitudes in many substances. The large discrepancy in C—H amplitudes depends on the experimental background curve. In the absence of primary experimental data, we had no way of refining the background and therefore had to assume a fixed (reasonable) value for the C—H amplitude. A large discrepancy between the experimental and calculated $f(r)$ curves is also observed in the range $r = 4$ to $r = 6$ Å, possibly for the same reason. However, in the middle range, agreement between experimental and calculated $f(r)$ curves is very good.

The ab initio prediction for the P—F bond length, 1.60 Å, is much longer than that found by Zeil et al., 1.54 Å, or the average

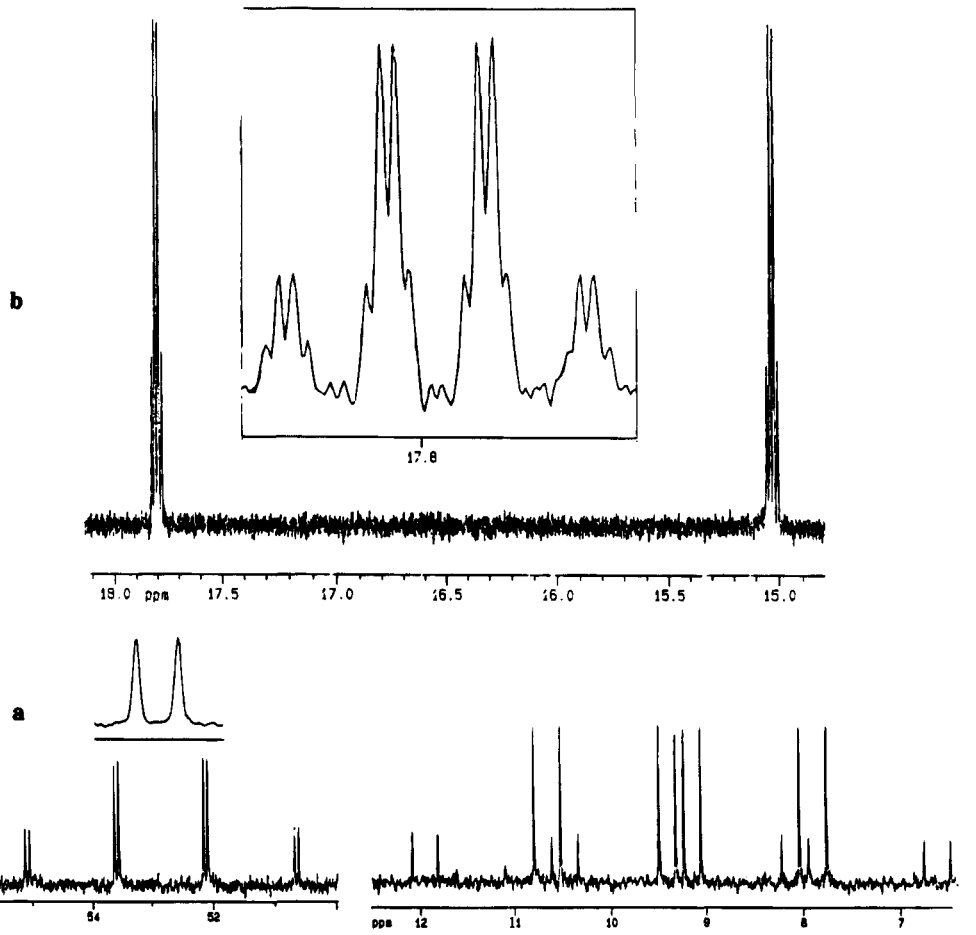


**Figure 3.** NMR spectra of **1**: (a) $^{13}C$ NMR spectrum with the proton-decoupled spectrum of MeO carbon shown above; (b) $^{19}F$ NMR spectrum with the expanded low-field signal shown above.

value of the P−F bond length in related compounds, 1.52 Å.[23] A lengthening is expected on the basis of the anomeric effect which involves electron transfer into the P−F antibonding orbital, but perhaps the effect is exaggerated at both the MP2/6-31G(D) and Becke3LYP/6-31G(D) levels.

Experience with GED analysis has shown that the inner part of the scattering pattern is subject to large uncertainties. Accordingly, we repeated the refinements using the range $S_{min} > 3.6$ Å$^{-1}$ rather than $S_{min} > 1.0$ Å$^{-1}$. In this case, we constrained only the difference between the P=O and C−O bond lengths according to the ab initio calculations and treated $r$(P−F) and (P−O) as independent parameters. The results of these refinements for the three model structures of Chart 1 are presented as the last three columns of Table 2. The least squares standard deviations are given in parentheses as units in the last digit(s). The largest coefficients of correlation are the following: ($r$(P=O)/$r$(P−F)) 0.96; ($r$P=O)/∠OPO) 0.81; ($r$(P−O/∠O=PF) 0.86; (∠O=PF/∠CPOC) 0.90. Such large correlations between parameters do not permit a detailed discussion of structural peculiarities. The new radial distribution curve (E) and the difference curves (E − T) show better agreement between experiment and theory (Figure 4b), and the $R$-factors, given in Table 2, are significantly decreased (about 5%). However, the differences among the $R$-factors for the different conformations are statistically insignificant. The present analysis strongly suggests that GED experiments cannot determine which of the conformations of **1** is the major one.

**Electronic Structure and Chiroptical Properties.** The UV absorption spectrum of **1** shows no maximum in the accessible spectral range, >190 nm. The CD spectra of sarin (**2**) and soman (**3**) do not exhibit any Cotton effects (CEs) in the same spectral range. We have applied the PCI program to examine the nature of the lower-lying electronic states of **1** and have predicted the energies, $\Delta E$, electric dipole oscillator strengths, $f$, and optical rotatory strengths, [$R$], for transitions to these states. The results are collected in Table 3. The lowest electronic excitation energy is predicted to be almost 10 eV. It is well known that a single-CI treatment will overestimate the excitation energy because it does not allow for relaxation of the "unexcited" electrons. However, even if the error were as large as 2−3 eV, it is clear that no electronic absorption is predicted in the normally accessible UV region (>180 nm, <6.9 eV). In addition, all of the first few transitions are predicted to have relatively low oscillator strengths. However, the first two electronic transitions of both conformers are predicted to have moderate rotatory strengths of the same sign, (+ve for (*R*)-**1**). On this basis, one would expect positive optical rotation for (R)-**1** at longer wavelengths as well; i.e., the absolute configuration is tentatively assigned as (+)-(*R*)-**1**.

The expectation values, $\langle r^2 \rangle$, for the higher singly occupied MO as derived by the CI calculations are also given in Table 3. These serve as indicators of the character (valence or Rydberg) of the electronic state. A small value of $\langle r^2 \rangle$ indicates a valence (compact) excited state whereas a larger value indicates Rydberg (diffuse) character to the excited state. As can be seen from Table 3, these expectation values, which are in units of bohr$^2$ (0.529 17 Å = 1 bohr), suggest an average separation of the electron from the molecular center of about 3 Å, and therefore imply considerable Rydberg character to all

(23) Carlowitz, S. v.; Zeil, W.; Pulay, P.; Boggs, J. E. *J. Mol. Struct.* **1982**, *87*, 113−124.

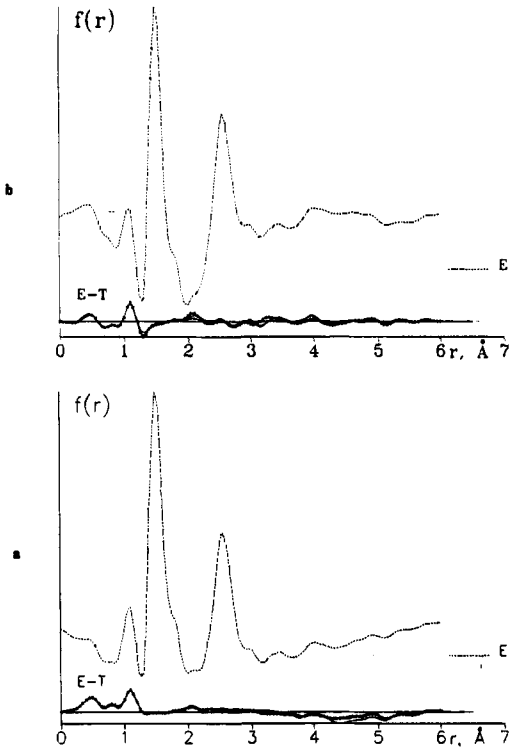


**Figure 4.** Experimental (E) radial distribution curve ($f(r)$) and three difference curves (E − T), where T represents the theoretical $f(r)$ for the three models (**a**, **b**, and **c** in Chart 1): (a) the full $sM_{(s)}$ curve; (b) the shortened $sM_{(s)}$ curve (see text).

**Table 3.** Calculated Electronic Properties for (*R*)-**1a** and (*R*)−**1b**

| property[a] | (*R*)-**1a** | (*R*)-**1b** | property[a] | (*R*)-**1a** | (*R*)-**1b** |
|---|---|---|---|---|---|
| | | $S_0-S_1$ ($n_O-3s$) | | | |
| *E*, eV | 9.88 | 9.90 | *f* | 0.006 | 0.005 |
| $[R]^r$ | +5.1 | +15.5 | $\langle r^2\rangle$ | 30.2 | 31.8 |
| $[R]^\nabla$ | +5.3 | +13.1 | | | |
| | | $S_0-S_2$ ($n'_O-3s$) | | | |
| *E*, eV | 10.06 | 10.29 | *f* | 0.046 | 0.168 |
| $[R]^r$ | +23.4 | +5.8 | $\langle r^2\rangle$ | 29.0 | 30.7 |
| $[R]^\nabla$ | +21.5 | +4.2 | | | |
| | | $S_0-S_3$ (n−3p) | | | |
| *E*, eV | 10.67 | 10.47 | *f* | 0.006 | 0.005 |
| $[R]^r$ | −4.5 | −10.8 | $\langle r^2\rangle$ | 33.0 | 33.2 |
| $[R]^\nabla$ | −5.5 | −9.6 | | | |
| | | $S_0-S_4$ (n−3p) | | | |
| *E*, eV | 10.79 | 10.67 | *f* | 0.005 | 0.005 |
| $[R]^r$ | −15.0 | −1.1 | $\langle r^2\rangle$ | 29.2 | 21.9 |
| $[R]^\nabla$ | −15.2 | −2.1 | | | |

[a] *E* = vertical excitation energy; $[R]^r$ = optical rotatory strength in the length formulation, in units of $10^{40}$ cgs; $[R]^\nabla$ = optical rotatory strength in the velocity formulation; *f* = oscillator strength; $\langle r^2\rangle$ = expectation value of $r^2$ with respect to the upper singly occupied orbital of the excited state, in units of bohr$^2$.

four of the lower excited singlet states. The states originate by electron excitation from the highest occupied molecular orbital (HOMO) ($S_1$), from HOMO − 1 ($S_2$), or from linear combinations of the two ($S_3$, $S_4$). The HOMO and HOMO − 1 are predominantly the two nonbonded 2p orbitals on the monocoordinated oxygen atom (Figure 5). The higher singly occupied orbitals of $S_1$ and $S_2$ are essentially identical (except for phase) and correspond to a molecular 3s orbital largely centered on the monocoordinated oxygen atom (Figure 5).

## Conclusions

By applying electronic structure theory at the MP2/6-31G(D) and Becke3LYP/6-31G(D) levels, we have confirmed the prior results of lower-level ab initio calculations[7] which indicated that the experimental GED structure[5] of *O*-methyl methylphosphonofluoridate (**1**) is substantially in error. The compound exists essentially in a single conformation, **1a**, determined by the operation of an anomeric effect between the methoxy oxygen atom and the P−F bond as is evident from the nearly perpendicular orietnation of the O−C and P−F bonds (88.2° and 90.2° at MP2 and Becke3LYP, respectively). An attempt at reanalysis of the published GED data yielded inconclusive results but reconfirmed the difficulties arising from very similar values of the bonds between the heavy atoms. The $^1$H and $^{13}$C NMR spectra are consistent with the existence of a single conformer, and the absence of $^3J_{CF}$ spin−spin coupling implies a nonplanar geometry. The lower excited singlet states of **1** are calculated to be Rydberg states originating from excitations from the p−type lone pair orbitals of the monocoordinated oxygen atom into diffuse 3s- and 3p-type orbitals. The transitions are predicted to occur in the vacuum UV and have low oscillator strength. The first two transitions have moderate positive rotatory strength for the (*R*) enantiomer, leading to the prediction of absolute configuration, (+)-(*R*)-**1**.

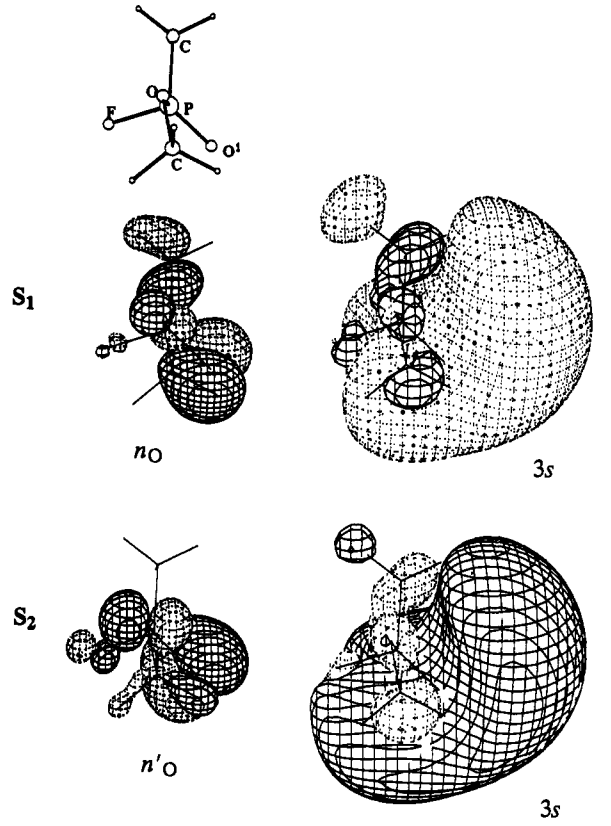


**Figure 5.** Singly occupied molecular orbitals of the first excited singlet state, $S_1$, and the second, $S_2$. $n_O$ = MO 29 (HOMO), $n'_O$ = MO 28 (HOMO − 1), and the contour value is 0.05; the 3s Rydberg orbitals are plotted at contour 0.02.

**Acknowledgment.** We thank the Natural Sciences and Engineering Research Council of Canada for financial support of this work. Partial funding was also provided by NATO in the form of a Linkage Grant, and the International Science Foundation (Grant No. MQX000). I.F.S. and L.V.V. acknowledge financial support from the Russian Foundation of Fundamental Research (Grant No. 93-03-4410).

JA950261M